Angewandte International Edition Chemie

DOI: 10.1002/anie.201006065

Agostic Alkyl Complexes

The Nature of β-Agostic Bonding in Late-Transition-Metal Alkyl Complexes**

Wolfgang Scherer, Verena Herz, Andreas Brück, Christoph Hauf, Florian Reiner, Sandra Altmannshofer, Dirk Leusser, and Dietmar Stalke*

In general, C–H bonds can be considered chemically inert as a result of their strength, nonpolar nature, and low polarizability. Since the pioneering work of La Placa and Ibers in 1965, who reported the close approach of a C–H bond to a transition-metal center, there have been many attempts to trace the microscopic control parameters of such C–H activation processes by metal atoms in general.[1] In particular, complexes containing side-on-coordinated (η^2-CH) moieties next to a transition metal are the focus of intensive research as they allow the systematic study of the C–H activation phenomenon in molecules and solids in their electronic ground states. Furthermore, M···H–C interactions (M = transition metal) play a key role in the performance of several industrially relevant catalytic processes, such as olefin polymerization.[2]

In the course of a systematic analysis of such M···H–C interactions, Brookhart and Green coined the expression agostic interactions to "*discuss the various manifestations of covalent interactions between C–H groups and transition-metal centers in organometallic compounds*".[3a,b] In case of d^0 early-transition-metal alkyl or amido complexes, the strength of agostic interactions is mainly controlled by 1) the local Lewis acidity of the metal center, 2) the extent of negative hyperconjugative delocalization of the M–C/M–N bonding electrons, and 3) to a smaller degree by σ(M←H–C) donation.[3c,4] For agostic late-transition-metal complexes, however, the control parameters are less clear. We therefore synthesized a variety of new Spencer-type[5] nickel alkyl cations **2b**–**d** by protonation of the corresponding olefin complexes **1b**–**d** to study the nature of their pronounced agostic interactions by combined experimental and theoretical charge density studies (Scheme 1).

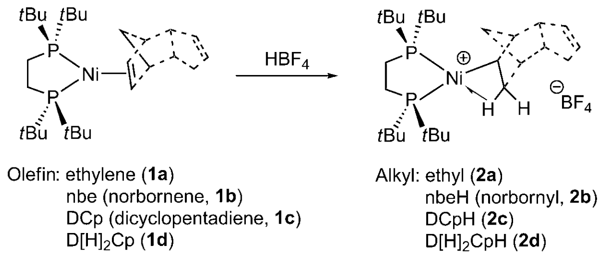

Scheme 1. Protonation of the olefin complexes **1a**–**d** yielding the corresponding agostic alkyls **2a**–**d**. D[H$_2$]Cp = dihydrodicyclopentadienyl.

Re-examination of the classic Spencer-type complex $[\mathrm{EtNi}(\mathrm{d}t\mathrm{bpe})]^+[\mathrm{BF_4}]^-$ (d*t*bpe = $t\mathrm{Bu_2PCH_2CH_2P}t\mathrm{Bu_2}$) (**2a**) showed a fast rotation of the β-agostic methyl moiety in solution ($\Delta H^{\ddagger} = (35.1 \pm 1.0)\ \mathrm{kJ\,mol^{-1}}$, $\Delta S^{\ddagger} = (-16 \pm 193)\ \mathrm{J\,mol^{-1}\,K^{-1}}$, $E_A = (37.0 \pm 1.0)\ \mathrm{kJ\,mol^{-1}}$)[6] and a systematic crystallographic disorder in the solid state, thus preventing a detailed investigation of the bonding properties of this agostic textbook example by experimental charge-density studies. We therefore replaced the ethylene moiety in **1a** by the sterically more demanding norbornyl (nbe) and dicyclopentadienyl (DCp) ligands. Protonation of **1b**–**d** yielded the agostic complexes **2b**–**d**, which all have a significantly reduced fluxional behavior in solution. Furthermore, single crystals of excellent quality could be obtained for **2b**–**d**, which even allowed an experimental charge-density analysis of **2c**.[7a–e]

The ^{1}H NMR signals of the agostic hydrogen atoms (Table 1) in **2b**–**d** do not shift significantly upon cooling, in contrast to **2a**.[6] Thus, fluxional processes involving 1) the rotation of the β-agostic alkyl moiety and/or 2) a combined β-elimination/alkene rotation seem to play only a minor role in our benchmark systems **2b**–**d** (Scheme 2), if at all. The latter process, however, appears to be important in case of agostic platinum diphosphine norbornyl complexes, such as $[(\mathrm{nbeH})\mathrm{Pt}(\mathrm{d}t\mathrm{bpe})]^+[\mathrm{BPh_4}]^-$ (**4b**), and to a lesser extent for its Pd analogue **3b**.[5a] In case of the agostic ethyl cations $[\mathrm{EtM}(\mathrm{d}t\mathrm{bpe})]^+$ (M = Ni (**2a**), M = Pd (**3a**), M = Pt (**4a**)), DFT calculations confirm Spencer's findings[5b,c] that the *cis* ethene

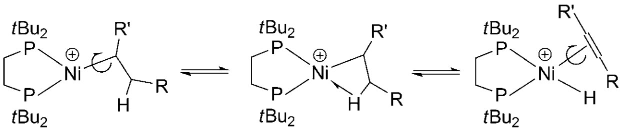

Scheme 2. Possible dynamical processes of **2a**–**d** in solution.

---

[*] Prof. Dr. W. Scherer, V. Herz, Dr. A. Brück, C. Hauf, F. Reiner, Dr. S. Altmannshofer
Institut für Physik
Lehrstuhl für Chemische Physik und Materialwissenschaften
Universität Augsburg, 86135 Augsburg (Germany)
Fax: (+49) 821-598-3227
E-mail: wolfgang.scherer@physik.uni-augsburg.de
Dr. S. Altmannshofer, Dr. D. Leusser, Prof. Dr. D. Stalke
Institut für Anorganische Chemie
Georg-August-Universität Göttingen
Tammannstrasse 4, 37077 Göttingen (Germany)

[**] This work was supported by the DFG (SPP1178) and NanoCat (an International Graduate Program within the Elitenetzwerk Bayern).

Supporting information for this article is available on the WWW under http://dx.doi.org/10.1002/anie.201006065.

Table 1: Experimental and calculated ^{1}H NMR chemical shifts δ ([ppm], $\delta = \sigma(\text{TMS}) - \sigma$ with $\sigma^{\text{calc}}(\text{TMS}) = 31.59$ ppm), diamagnetic (σ^d) and paramagnetic ($\sigma^{p'}$) shielding contributions, and atomic charges Q^H_{AIM} of the corresponding agostic protons (see the Supporting Information).

	$\measuredangle$MCC$_\beta$ [°]	d(M−H) [Å]	δ [ppm]	σ^d [ppm]	$\sigma^{p'}$ [ppm]	Q^H_{AIM} [e]
2a[a]	74.5(3)	1.64(2)	−5.75[b]	–	–	–
DFT[c]	76.2	1.682	−3.78	28.16	7.21	−0.05
DFT[d]	75.0	1.634	−6.06	28.21	9.44	−0.05
DFT[e]	73.9	1.589	−9.59	28.02	13.17	−0.05
2b	74.2(1)	1.64(4)	−5.05	–	–	–
2c	74.92(3)	1.671(9)	−5.37[f]	–	–	−0.01
DFT	74.96	1.653	−5.62	28.43	8.78	−0.04
2d	74.6(1)	1.72(3)	−5.38	–	–	–
$\mathbf{7}_{\text{DFT}}$	84.4	2.029	−1.30	29.25	3.64	−0.10
5	84.4(1)[g]	2.10[g]	2.7[h,i]	–	–	0.13
DFT[j]	87.2	2.200	4.77	27.47	−0.65	−0.02
DFT[k]	85.1	2.110	5.10	27.64	−1.16	−0.03
DFT[l]	82.5	2.000	5.48	28.00	−1.90	−0.04

[a] Ref. [5c]. [b] At 183 K. [c–e] Relaxed PES scan with Ni−P$_{trans}$ = 2.0, 2.156 (equilibrium geometry), and 2.4 Å, respectively. [f] Average value (two diastereomers in solution; individual values: −5.27/−5.46 ppm). [g] Ref. [4c], [8a]. [h] Averaged signal owing to methyl group rotation. [i] Ref. [8b,c]. [j–l] Relaxed PES scan with a variable Ti−H distance of 2.2, 2.11 (equilibrium geometry), and 2.0 Å, respectively.

hydride form is favored in case of the Pt complex **4a** (0.2 kcal mol^{-1}) versus the agostic structure, while the latter is preferred by the palladium analogue **3a** by 5.2 kcal mol^{-1}. In case of **2a**, the *cis* ethene hydride form does not even represent an energetic minimum on the potential energy surface (PES) but a transition state (14.8 kcal mol^{-1} above the agostic equilibrium geometry), with the olefin moiety aligned perpendicular to the NiP$_2$H plane. The restricted fluxionality of nickel complexes **2b–d** versus the norbornyl Pd and Pt complexes allowed the determination of the geminal $^2J_{\text{HH}}$ coupling constants (16.2–17.4 Hz) and the surprisingly large $^2J_{\text{HP}}$ (30.0–31.1 Hz) coupling constants between the agostic proton and the phosphorous nuclei in the *trans* position. This result indicates the importance of the electronic influence of the ligand *trans* to the agostic hydrogen atom as potential control parameter of the strength of the metal-mediated C−H activation.[4c]

Figure 1 shows the salient structural features of the d^{10} nickel olefin complex **1c** in comparison with its protonated form, the agostic d^8 nickel alkyl cation **2c**.[7a–e] Protonation causes only a subtle elongation by 0.053 [0.058] Å of the olefinic C−C double bond. (Theoretical values obtained by DFT calculations employing the scalar ZORA Hamiltonian at the BP86/TZ2P level of approximation[7f,g] are given in square brackets.) The short Ni−H$_\beta$ bond (1.671(9) [1.653] Å) also classifies **2c** as an agostic benchmark system close to the *cis* ethene hydride form that represents the termination of the β elimination pathway. Indeed, the observed and calculated Ni−H$_\beta$ bond lengths in **2c** approach the characteristic values of covalent nickel(II) hydrides; for example, Ni−H 1.46(3) Å in [(η^5-C$_5$Me$_5$)Ni(PEt$_3$)H].[9] Furthermore, the strength of the Ni−H bond is reflected by a significant electron-density accumulation at the Ni−H$_\beta$ bond critical point (BCP) of 0.553(4) [0.569] e Å^{-3}, which approaches the values at the Ni−C$_\alpha$ BCP (0.680(9) [0.735] e Å^{-3}), which is our internal standard of a covalent nickel–ligand bond. However, the 1) large bond ellipticities ε, 2) small negative value of the total energy density $H(\mathbf{r})$, and 3) high density accumulation also at the ring critical point (RCP) inside the {NiC$_\alpha$C$_\beta$H$_\beta$} fragment reveals that the remarkable covalent character of the Ni−H$_\beta$ bond has not been fully developed (Table 2).

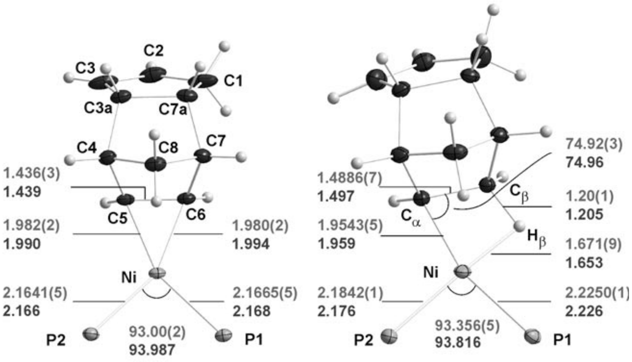

Figure 1. ORTEP representations (ellipsoids set at 50% probability) of the d^{10} nickel olefin complex **1c** and the protonated agostic d^8 cation **2c** at 100 K. Salient bond distances [Å] and angles [°] are shown; theoretical values are given below the experimental values.

Table 2: Selected topological parameters ($\rho(\mathbf{r})$ [e Å^{-3}], $\nabla^2\rho(\mathbf{r})$ [e Å^{-5}], ε, $H(\mathbf{r})$ [hartree Å^{-3}], and $G(\mathbf{r})/\rho(\mathbf{r})$ [hartree e^{-1}]) at the bond and ring critical points in the agostic {NiC$_\alpha$C$_\beta$H$_\beta$} fragment of **2c**.

Unit		$\rho(\mathbf{r}_c)$	$\nabla^2\rho(\mathbf{r}_c)$	ε	$H(\mathbf{r}_c)$	$G(\mathbf{r}_c)/\rho(\mathbf{r}_c)$
Ni−C$_\alpha$	Expt	0.680(9)	7.5(1)	0.78	−0.247	1.137
	DFT	0.735	4.0	0.21	−0.286	0.769
C$_\alpha$−C$_\beta$	Expt	1.77(2)	−12.6(1)	0.11	−2.384	0.847
	DFT	1.700	−12.7	0.12	−1.417	0.309
C$_\beta$−H$_\beta$	Expt	1.33(3)	−5.1(1)	0.15	−1.407	0.789
	DFT	1.387	−11.6	0.07	−1.157	0.251
H$_\beta$−Ni	Expt	0.553(4)	6.2(1)	1.58	−0.154	1.069
	DFT	0.569	6.3	0.96	−0.180	1.089
RCP	Expt	0.533	6.3	–	−0.134	1.080
	DTF	0.507	6.5	–	−0.105	1.098

As a consequence, both experimental and theoretical charge density studies reveal a stable C$_\beta$−H$_\beta$ bond path, which however shows a significantly diminished charge density accumulation at its BCP of $\rho(\mathbf{r})_{\text{C-H}} = 1.33(3)$ [1.387] e Å^{-3} (Table 2) relative to the weakly activated C−H bonds displayed by our agostic reference systems of early-transition-metal alkyl compounds (for example [EtTiCl$_3$(dmpe)] (**5**; dmpe=(CH$_3$)$_2$PCH$_2$CH$_2$P(CH$_3$)$_2$); $\rho(\mathbf{r})_{\text{C-H}} = 1.54(5)$ [1.685] e Å^{-3}).[4c]

The same conclusion also holds for so-called lithium agostic systems (for example in [{2-(Me$_3$Si)$_2$CLiC$_5$H$_4$N}$_2$] (**6**), $\rho(\mathbf{r})_{\text{C-H}} = 1.71(6)$ [1.770] e Å^{-3})[4a,b] where the M···H−C bonding can be considered as a secondary, weak electrostatic interaction. As a surprising result of the dramatically reduced density accumulation in the C$_\beta$−H$_\beta$ bonding region of **2c**, we could freely refine the respective C$_\beta$−H$_\beta$ bond distance of

1.20(1) Å, in good agreement with the DFT calculations [1.205 Å], simply by considering the dipolar polarization of $\rho(\mathbf{r})$ of the agostic hydrogen atom by its bonding partners (Ni and C_β) in the multipolar model.

Accordingly, **2c** complements the small series of C–H agostic benchmarks characterized by experimental charge-density studies (**5** and **6**) and can be employed to validate the numerous theoretical studies in this field. In this respect **2c** and **5** are characteristic test beds for agostic systems displaying either strongly (late-transition-metal alkyls) or moderately (early-transition-metal alkyls) activated C–H bonds, while the main group alkyl **6** shows the characteristic features of systems establishing merely electrostatic M···H–C contacts.

The need for a classification/discrimination of agostic interactions is also supported by our experimental and theoretical NMR studies (Table 1). For the calculation of chemical shifts and shielding contributions with the ADF NMR property program, the spin–orbit ZORA-Hamiltonian at the hybrid PBE0/TZ2P level of approximation was employed.[7h] Thus, the calculated isotropic shielding values consist of three contributions: the diamagnetic (σ^{d}), paramagnetic (σ^{p}), and spin–orbit (σ^{so}) term. As the σ^{so} contribution is usually small, we only report the sum $\sigma^{\mathrm{p}'} = \sigma^{\mathrm{p}} + \sigma^{\mathrm{so}}$ (for individual values, see the Supporting Information). We previously pointed out that agostic d^0 transition-metal alkyls such as **5** or amido complexes are not necessarily characterized by an upfield shift of the ^{1}H NMR signal of the agostic protons.[4g] This fact is in conflict with the general presumption that agostic protons are significantly shielded as a consequence to their proximity to the metal center and their partial hydridic character. Accordingly, the assumed gain in electron density owing to agostic interactions should result in an increase of σ^{d}, corroborated by an upfield shift of the ^{1}H NMR signal. This generally accepted assumption is, however, not supported by any our detailed experimental and theoretical charge density analyses and NMR spectroscopy studies. Indeed, the atomic charges (Q_{AIM}) of all our model systems in Table 1 show a rather small variation of roughly $-0.1 < Q^{\mathrm{H}}{}_{\mathrm{AIM}} < 0.1\,\mathrm{e}$, in line with a correspondingly small change of the computed σ^{d} values in **2a**–**7**. Accordingly, the expression "hydridic shift", which is often used to correlate the chemical shifts with the charge density accumulation at the metal bonded hydrogen atoms, appears to be misleading in the case of agostic hydrogen atoms. Analysis of the individual contributions to the isotropic shielding $\sigma = \sigma^{\mathrm{d}} + \sigma^{\mathrm{p}'}$ shows that the ^{1}H NMR chemical shifts for the agostic protons depend mainly on the sign and magnitude of $\sigma^{\mathrm{p}'}$.

Interestingly, the magnitude and sign of $\sigma^{\mathrm{p}'}$ does not depend on the presence or absence of free d electrons, as exemplified by the large $\sigma^{\mathrm{p}'}$ values for our cationic d^0 model system $[\mathrm{EtTiCl_2}]^+$ (**7**) ($\sigma^{\mathrm{p}'}_{\mathrm{calc}} = +3.64$ ppm) and its corresponding d^8 system $[\mathrm{EtNi(d}^t\mathrm{bpe)}]^+$ ($\sigma^{\mathrm{p}'}_{\mathrm{calc}} = +9.44$ ppm), while the neutral d^0 benchmark **5** has a negative $\sigma^{\mathrm{p}'}_{\mathrm{calc}}$ value (-1.16 ppm), in line with a downfield ^{1}H shift and the observation of a negative isotopic perturbation of resonance (IPR) in experimental NMR spectroscopy studies.[8a] Subsequent detailed analyses of the calculated chemical shifts of the agostic proton in **2a** reveal an interesting *trans* influence: a subtle and stepwise weakening of the Ni–P bond *trans* to the agostic proton is paralleled by a subtle shortening of M–H distances and a large upfield shift of the ^{1}H NMR signal of the agostic proton (Table 1). The charge at the agostic hydrogen atoms remains rather invariant upon this geometrical change and the same is consequently true for the diamagnetic shielding contribution. Indeed, our studies show that the upfield shift in **2a** is due to the pronounced increase of $\sigma^{\mathrm{p}'}$ (Table 1). It might be supposed that it is the metal-to-hydrogen distance that mainly controls the sign and magnitude of the $\sigma^{\mathrm{p}'}$ contribution. However, the results depicted in Table 1 clearly rule out this simple assumption. Indeed, the early-transition-metal d^0 complex **5** shows the reverse trend and has a downfield shift upon shortening the Ti···H distance. The same trend has been also observed in an earlier study of agostic early-transition-metal amido d^0 complexes.[4g] In the molecular orbital (MO) picture paramagnetic shielding originates from a mixing of ground and excited states in the presence of the applied external magnetic field. It is therefore not surprising that the prediction of sign and magnitude of $\sigma^{\mathrm{p}'}$ usually warrants detailed MO analyses.[10]

In case of agostic d^0 type complexes, we noted already that the local Lewis acidity of the central metal atoms plays a crucial role in the C–H activation step and might also influence the ^{1}H NMR spectroscopic properties of the agostic proton.[4g] As a consequence of the covalent Ni–C_α and Ni–H_β interactions in the agostic Ni d^8 systems **2a**–**d**, the Ni($d_{x^2-y^2}$) orbital (which is involved simultaneously in both interactions) becomes significantly depopulated relative to the other d orbitals (for a definition of the coordinate system see Figure 2a). This effect is supported by the relatively small $P(d_{x^2-y^2})$ population of only 1.62(2) e derived from our experimental multipole model (see the Supporting Information). As a consequence, the fine structure of the negative Laplacian of the charge density, $-\nabla^2\rho(\mathbf{r}) = L(\mathbf{r})$, of **2c** displays four pronounced charge-depletion (CD) zones in the valence shell charge concentration (VSCC) of the nickel atom along the local x,y coordinate axes. As the four CD zones (denoted CD1–4 in Figure 2a) in the charge-density picture are directly connected with the depletion of the metal $d_{x^2-y^2}$ orbital in the MO picture, the angle between these CD zones is constrained and dictates the position of all ligand atoms in a key-and-lock scenario. Indeed, the metal-directed VSCC of each ligand L atom faces one of the four CD zones (representing a local Lewis acidic center) at the metal atom (Figure 2a). Analysis of the molecular orbitals of the $[\mathrm{EtNi}]^+$ cation shows that the depletion of the $d_{x^2-y^2}$ orbitals is a consequence of the Ni→L π back-donation (HOMO−4 in Figure 2b). Owing to the symmetry restraints imposed by the nodal plane (which is oriented perpendicular to the molecular plane and parallel to the Ni···C_β vector), HOMO−4 contributes simultaneously to covalent Ni–C_α, C_α–C_β, and Ni–H_β bonding. The agostic interaction is further established by additional Ni←L π (HOMO−6) and σ donation (HOMO−7). Accordingly, the bonding in β-agostic late-transition-metal complexes can be considered in terms of an adopted Dewar–Chatt–Duncanson (DCD) model. The additional Ni←L π donation (which complements the σ-donation and π-back-donation component in the classical DCD model for olefin complexes) reflects the increased functionality of β-agostic

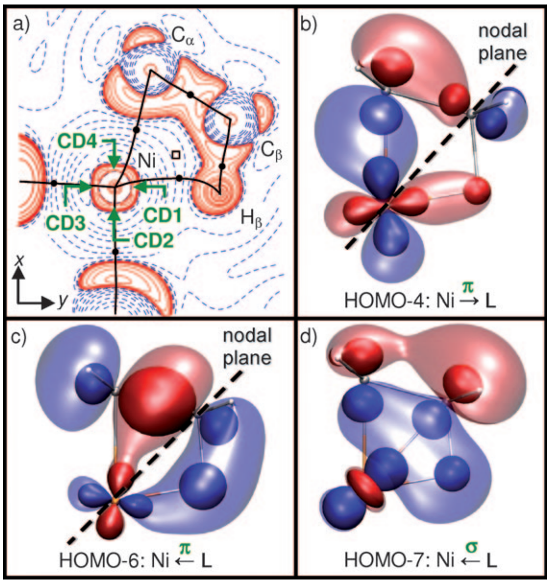

Figure 2. a) Experimental contour map of $L(\mathbf{r}) = -\nabla^2\rho(\mathbf{r})$ and bond paths (black solid line) in the agostic $\{NiC_\alpha C_\beta H_\beta\}$ moiety of **2c**. Positive (solid) and negative (dashed) contour lines are drawn at 0, $\pm 2.0\times 10^n$, $\pm 4.0\times 10^n$, $\pm 8.0\times 10^n$ e$Å^{-5}$ with $n = \pm 3, \pm 2, \pm 1, 0$; one contour level deleted (800 e$Å^{-5}$); extra level at 30 and 1100 e$Å^{-5}$. b–d) Multicenter molecular orbitals in the $[EtNi]^+$ cation (isodensity map at 0.05 a.u.) establishing the Ni→L π back-donation, Ni←L π donation, and Ni←L σ donation, respectively (L = alkyl unit). The inner lobes are given schematically to clarify the salient atomic orbital contributions.

alkyl ligands by involving the β-H atom in the ligand-to-metal bonding.

In the next step of our analysis, we outline that the different bonding scenarios in the MO description of early and late-transition-metal complexes should be reflected by different VSCC patterns at the metal atoms. We also show that these experimentally observable differences in the VSCC topology can be correlated with the magnitude and sign of the $\sigma^{p'}$ contribution at the agostic proton. Indeed, inspection of the VSCC pattern of our model systems **2c**, **5**, and **7** reveals a clear topological trend (Figure 3a–c): large upfield shifts of the agostic proton are only observed in a topological scenario where the M···H bond path approximates a local charge depletion, a (3, +1) critical point (CP) at the metal center (**2a–d**; Figure 3a). The reverse scenario is found for our d^0 benchmark complex **5** where the computed Ti···H_β atomic interaction line is close to a local charge concentration, a (3,–3) CP (Figure 3c). In line with our hypothesis, a downfield shift of the agostic proton is experimentally observed and predicted by DFT.[8a] The theoretical model system **7** also follows this trend and marks an intermediate case between strong (**2a–d**) and weak agostic interactions (**5**). Indeed, in **7** the Ti···H bond path is close to a saddle point, a (3,–1) critical point in the $L(\mathbf{r})$ maps, while the C_β–H_β moiety is still facing a charge depletion zone. Accordingly, DFT predicts an upfield shift of the agostic proton (−1.3 ppm) and a C_β–H_β bond activation (ca. 0.06 Å), which are both intermediate between **5** (ca. +5.1 ppm and 0.03 Å, respectively) and **2a–d** (ca. −5.5 ppm and 0.1 Å, respectively).[11]

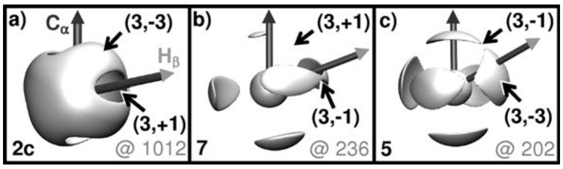

Figure 3. Envelope maps of $L(\mathbf{r})$ of **2c** (a), **7** (b), and **5** (c) at the corresponding metal atoms (the distance vectors towards the C_α and H_β atoms are marked by arrows; values are in given in e$Å^{-5}$).

In summary, our experimental charge-density analyses reveal significant differences between the nature of β-agostic bonding in early- and late-transition-metal complexes. These results are supported by MO analyses showing that the β-agostic phenomenon in d^0 complexes can be described by one molecular orbital that accounts for the hyperconjugative delocalization of the M–C_α bonding pair over the β-agostic alkyl backbone and the establishment of secondary M···H interactions.[4c,8a] In case of d^n-configurated complexes of late-transition-metal complexes, however, β-agostic interactions can be described in terms of an adopted Dewar–Chatt–Duncanson model. This model suggests three bonding components in case of our d^8 nickel alkyl reference systems: 1) Ni→L π back-donation, 2) Ni←L π donation, and 3) Ni←L σ donation. Accordingly, the ^1H NMR spectroscopic properties of the agostic proton in the d^0 and d^n systems differ clearly and can be correlated with the local topology of the valence shell charge concentration of the respective transition-metal centers. We showed that only in cases where the agostic hydrogen atom is facing a local Lewis acidic center (charge depletion zone) at the metal atom, large upfield shifts and highly activated C_β–H_β bonds are observed. We further clarified that the commonly used term "hydridic shift" to explain the upfield shift of agostic protons is misleading and is not necessarily correlated with the atomic charge at the agostic hydrogen atom.

Received: September 28, 2010
Published online: February 18, 2011

Keywords: agostic interactions · alkyl complexes · electron density · NMR spectroscopy · topology

---

[1] S. J. La Placa, J. A. Ibers, *Inorg. Chem.* **1965**, *4*, 778–783.

[2] See, for example: M. P. Mitoraj, A. Michalak, T. Ziegler, *Organometallics* **2009**, *28*, 3727–3733, and references therein.

[3] a) M. Brookhart, M. L. H. Green, *J. Organomet. Chem.* **1983**, *250*, 395–408; b) M. Brookhart, M. L. H. Green, L.-L. Wong, *Prog. Inorg. Chem.* **1988**, *36*, 1–124; for recent reviews see c) W. Scherer, G. S. McGrady, *Angew. Chem.* **2004**, *116*, 1816–1842; *Angew. Chem. Int. Ed.* **2004**, *43*, 1782–1806; d) E. Clot, O. Eisenstein, *Struct. Bonding (Berlin)* **2004**, *113*, 1–36; e) M. Brookhart, M. L. H. Green, G. Parkin, *Proc. Natl. Acad. Sci. USA* **2007**, *104*, 6908–6914; f) M. Etienne, J. E. McGrady, F. Maseras, *Coord. Chem. Rev.* **2009**, *253*, 635–646.

[4] a) W. Scherer, P. Sirsch, M. Grosche, M. Spiegler, S. A. Mason, M. G. Gardiner, *Chem. Commun.* **2001**, 2072–2073; b) W. Scherer, P. Sirsch, D. Shorokhov, G. S. McGrady, S. A. Mason, M. Gardiner, *Chem. Eur. J.* **2002**, *8*, 2324–2334; c) W. Scherer, P.

Sirsch, D. Shorokhov, M. Tafipolsky, G. S. McGrady, E. Gullo, *Chem. Eur. J.* **2003**, *9*, 6057 – 6070; d) L. Perrin, L. Maron, O. Eisenstein, M. F. Lappert, *New J. Chem.* **2003**, *27*, 121 – 127; e) D. A. Pantazis, J. E. McGrady, M. Besora, F. Maseras, M. Etienne, *Organometallics* **2008**, *27*, 1128 – 1134; f) S. Scheins, M. Messerschmidt, M. Gembicky, M. Pitak, A. Volkov, P. Coppens, B. G. Harvey, G. C. Turpin, A. M. Arif, R. D. Ernst, *J. Am. Chem. Soc.* **2009**, *131*, 6154 – 6160; g) W. Scherer, D. J. Wolstenholme, V. Herz, G. Eickerling, A. Brück, P. Benndorf, P. W. Roesky, *Angew. Chem.* **2010**, *122*, 2291 – 2295; *Angew. Chem. Int. Ed.* **2010**, *49*, 2242 – 2246.

[5] a) N. Carr, B. J. Dunne, L. Mole, A. Guy Orpen, J. L. Spencer, *J. Chem. Soc. Dalton Trans.* **1991**, 863 – 871; b) L. Mole, J. L. Spencer, N. Carr, A. G. Orpen, *Organometallics* **1991**, *10*, 49 – 52; c) F. M. Conroy-Lewis, L. Mole, A. D. Redhouse, S. A. Litster, J. L. Spencer, *J. Chem. Soc. Chem. Commun.* **1991**, 1601 – 1603.

[6] The activation parameters for internal methyl group rotation in **2a** were determined from VT NMR experiments in qualitative agreement with our DFT calculations. Accordingly, an averaged signal of $\delta = -1.24$ ppm (CD_2Cl_2) can be assigned to the agostic methyl group at 293 K, while measurements at 183 K yield a signal at $\delta = -5.75$ ppm of the agostic proton, in good agreement with computed ^{1}H NMR shifts ($\delta = -6.06$, 1.11, and 1.10 ppm) for the agostic and non-agostic protons, respectively (see the Supporting Information).

[7] a) **1a–d** and **2a–d** were synthesized according to modified literature methods (see Ref. [5] and the Supporting Information). Crystal data for **2c**: $M_r = 597.14$, 100(2) K (Ref. [7b]) with $Mo_{K\alpha}$ radiation ($\lambda = 0.71073$ Å): yellow cuboid, orthorhombic, space group $Pna2_1$, $a = 19.106(3)$, $b = 16.648(2)$, $c = 9.385(1)$ Å, $V = 2985.2(7)$ Å^3; $Z = 4$, $F(000) = 1280$, $D_{calc} = 1.329$ g cm^{-3}, $\mu = 0.80$ mm^{-1}. $R_{int}(F) = 0.0346$ for a total of 282120 reflections yielding 37567 unique reflections. This data set provided 94.6% completeness in $3° < 2\theta < 112°$ ($\sin\theta_{max}/\lambda = 1.167$ Å^{-1}). The deformation density was described by a multipole model (Ref. [7d]) in terms of spherical harmonics multiplied by Slater-type radial functions with energy-optimized exponents using the XD program (Ref. [7e]). The refinement of 705 parameters against 30581 observed reflections [$F_o > 3\sigma(F)$, $\sin\theta_{max}/\lambda = 1.11$ Å^{-1}] converged to $R_1 = 0.027$, $wR_2 = 0.039$, and a featureless residual density map with minimum and maximum values of 0.32/−0.23 e Å^3 (see the Supporting Information). CCDC 794360 (**1c**) and 793746 (**2c**) contain the supplementary crystallographic data for this paper. These data can be obtained free of charge from The Cambridge Crystallographic Data Centre via www.ccdc.cam.ac.uk/data_request/cif; b) D. Stalke, *Chem. Soc. Rev.* **1998**, *27*, 171 – 232; c) T. Kottke, D. Stalke, *J. Appl. Crystallogr.* **1993**, *26*, 615 – 619; d) N. K. Hansen, P. Coppens, *Acta Crystallogr. Sect. A* **1978**, *34*, 909 – 921; e) A. Volkov, P. Macchi, L. J. Farrugia, C. Gatti, P. R. Mallinson, T. Richter, T. Koritsanszky, XD2006; f) ADF2009.01, SCM, Theoretical Chemistry, Vrije Universiteit, Amsterdam, The Netherlands, http://www.scm.com; g) G. te Velde, F. M. Bickelhaupt, S. J. A. van Gisbergen, C. Fonseca Guerra, E. J. Baerends, J. G. Snijders, T. Ziegler, *J. Comput. Chem.* **2001**, *22*, 931 – 967, and references therein; h) M. Krykunov, T. Ziegler, E. van Lenthe, *J. Phys. Chem. A* **2009**, *113*, 11495 – 11500, and references therein.

[8] a) A. Haaland, W. Scherer, K. Ruud, G. S. McGrady, A. J. Downs, O. Swang, *J. Am. Chem. Soc.* **1998**, *120*, 3762 – 3772; b) Z. Dawoodi, M. L H. Green, V. S. B. Mtetwa, K. Prout, *J. Chem. Soc. Chem. Commun.* **1982**, 1410 – 1411; c) Z. Dawoodi, M. L. H. Green, V. S. B. Mtetwa, K. Prout, A. J. Schultz, J. M. Williams, T. F. Koetzle, *J. Chem. Soc. Dalton Trans.* **1986**, 1629 – 1637.

[9] P. L. Holland, M. E. Smith, R. A. Andersen, R. G. Bergman, *J. Am. Chem. Soc.* **1997**, *119*, 12815 – 12823.

[10] a) Y. Ruiz-Morales, G. Schreckenbach, T. Ziegler, *Organometallics* **1996**, *15*, 3920 – 3923; b) A. D. Buckingham, P. J. Stephens, *J. Chem. Soc.* **1994**, 2747 – 2759.

[11] The agostic proton in $[Cp_2Ti(CH_2CHMeCH_2CHMe_2)]^+$ has a signal in the ^{1}H NMR spectrum at $\delta = -3.43$ ppm. F. Sauriol, J. F. Sonnenberg, S. J. Chadder, A. F. Dunlop-Briere, M. C. Baird, P. H. M. Budzelaar, *J. Am. Chem. Soc.* **2010**, *132*, 13357 – 13370.